

Cell Metabolism, Volume 29

Supplemental Information

**Phosphoproteomics Reveals
the GSK3-PDX1 Axis as a Key Pathogenic
Signaling Node in Diabetic Islets**

Francesca Sacco, Anett Seelig, Sean J. Humphrey, Natalie Krahmer, Francesco Volta, Alessio Reggio, Piero Marchetti, Jantje Gerdes, and Matthias Mann

Supplementary material for Sacco et al.

Supplementary Figures

Figure S1, related to Figure 1

db/db mice are obese with respect to control mice. Box plot showing the quartile distribution of body weight (A) and plasma glucose (B) of db/db and control 13 weeks old mice.

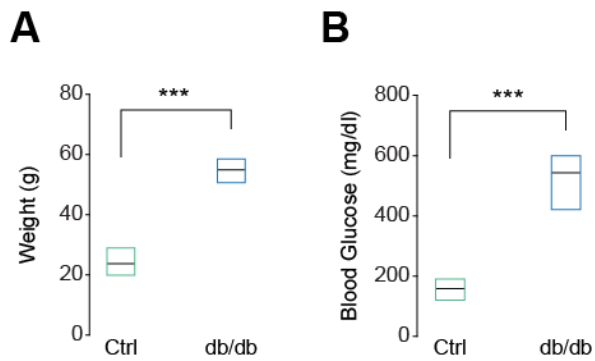


Figure S2, related to Figure 1

High coverage and reproducibility of proteome and phosphoproteome data. Number of quantified proteins (A) and phosphosites (B) in biological replicates of different experimental conditions. C) Venn diagram showing the proportion of class 1 sites in the whole quantified phosphosites. Heatmap showing the Pearson correlation coefficients between the different biological replicates in the proteome (D) and phosphoproteome (E) datasets.

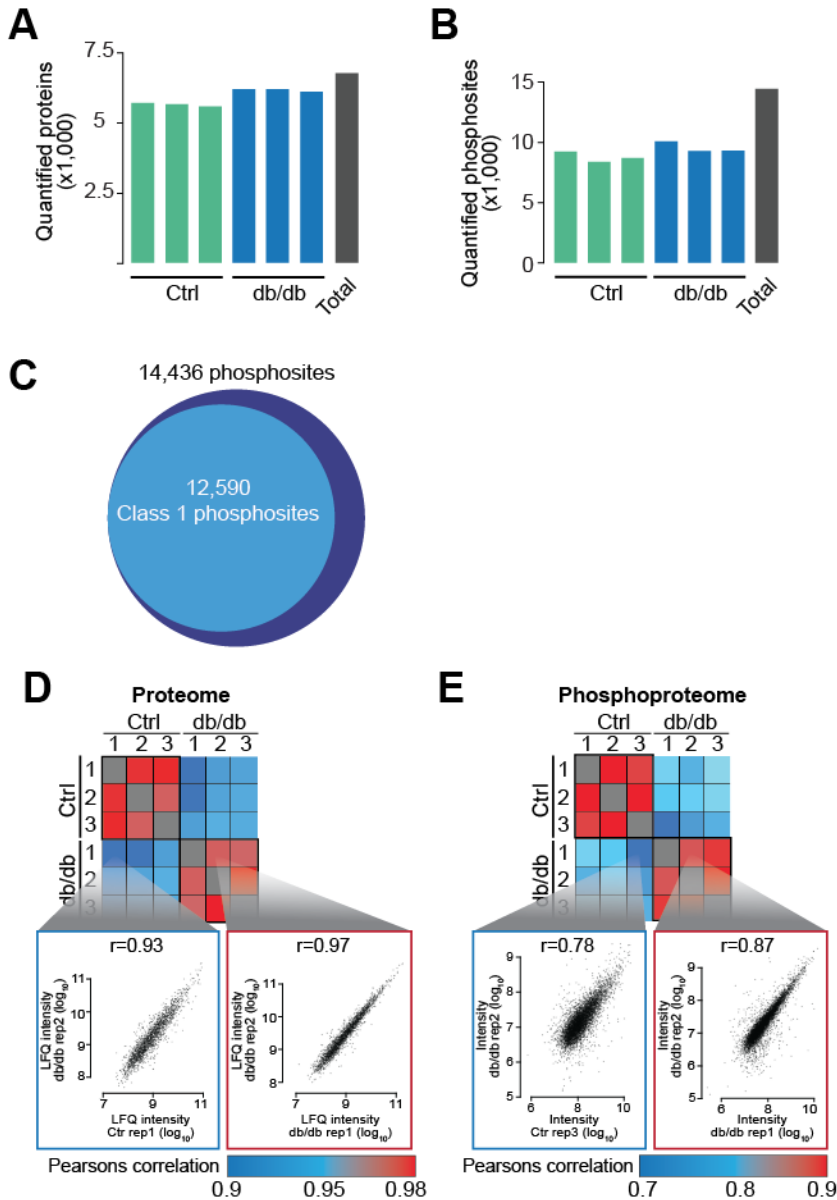


Figure S3, related to Figure 1

Data summary of the proteomic and phosphoproteomic data. **A)** Distribution of serine, threonine and tyrosine phosphorylation sites. **B)** Phosphosites quantified in our study that are already present in PhosphoSitePlus and annotated as “regulatory sites”. Phosphorylated proteins are distributed in the entire range of measured protein abundances. The distribution of ranked log₂ LFQ intensity values in control (**C**) and db/db islets (**D**) are colour-coded in grey, while phosphorylation intensity is in blue. **E)** Plot showing the distribution of the amplitudes (fold change of the log₂ intensities) calculated for the phosphoproteome (blue) as well as for proteome.

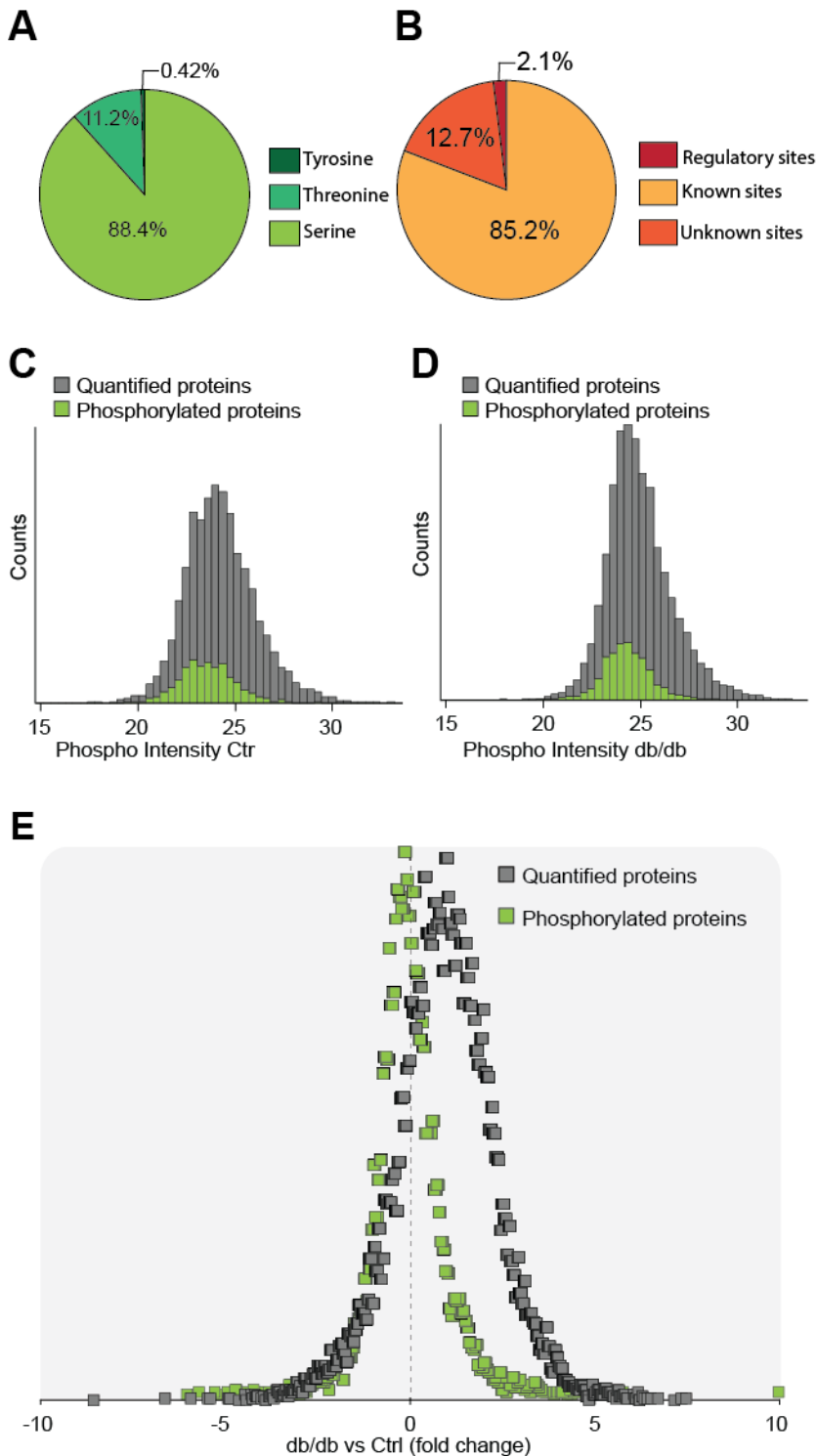


Figure S4, related to Figure 1

Comparison of proteins significantly modulated in db/db islets, with different T2D literature-derived datasets,

A) Venn diagram showing the overlap between the differentially expressed proteins derived by our and other proteomic approaches, as indicated. **B)** Multi-scatterplot showing the high correlation between fold changes of T2D-modulated proteins identified by different proteomic approaches. **C)** ER misfolded protein processing and degradation processes are schematically represented. Orange and red proteins are upregulated only in our db/db dataset and in at least 3 different T2D datasets respectively. **D)** Heatmap of protein expression level of genes significantly modulated in db/db islets and found to be significantly associated with T2D by GWAS studies.

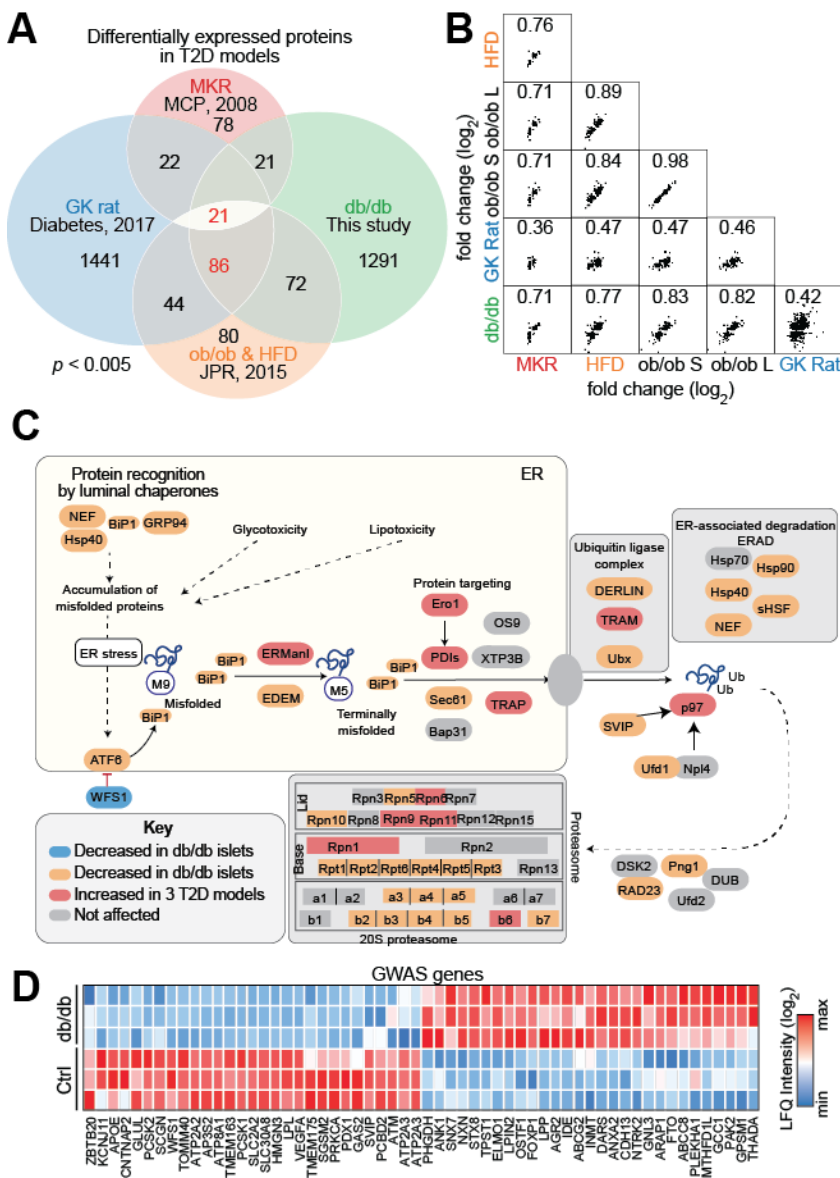


Figure S5, related to Figure 1

Proteomic comparison of islets derived from different T2D models A-B-C-D) Plots showing the correlation between our dataset and previously published proteomic datasets of islets from the indicated T2D murine and rat models (El Ouaamari et al., 2015; Hou et al., 2017; Lu et al., 2008). **E)** Heatmap of the 107 proteins significantly modulated in islets from at least three different T2D models.

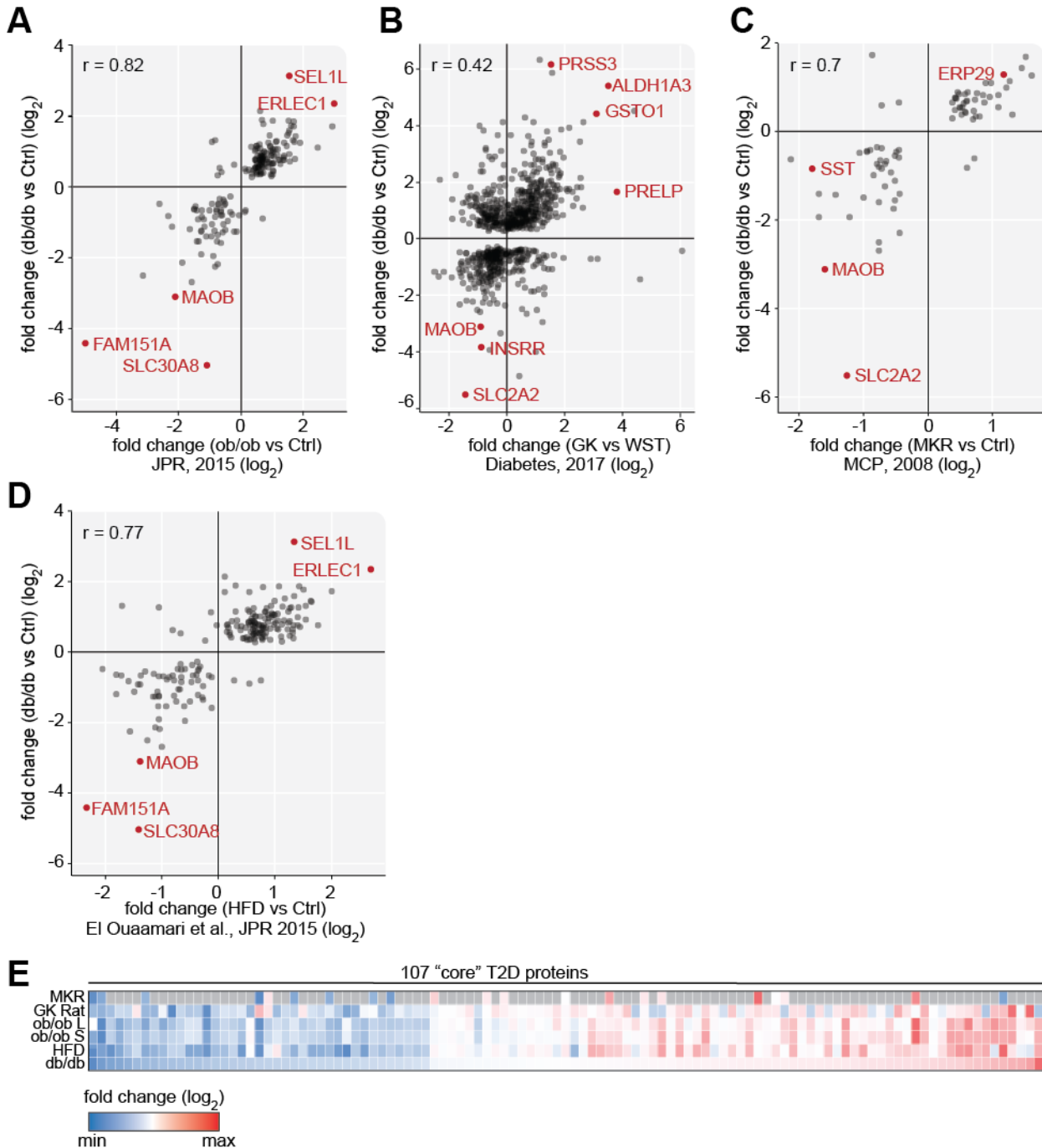


Figure S6, related to Figure 1

Comparison of transcriptome and proteome data on db/db islets. A) Plots showing the correlation between our dataset and the previously published transcriptome datasets of db/db islets (Neelankal John et al., 2018). **B)** Two-dimensional annotation enrichment analysis. Pathways modulated by metformin treatment at the proteome level in comparison with the transcriptome are plotted (FDR < 0.05). Each dot represents a specific KEGG pathway or GO-Biological Process (GO-BP) term. Groups of related pathways or GO-BP are labelled with the same color.

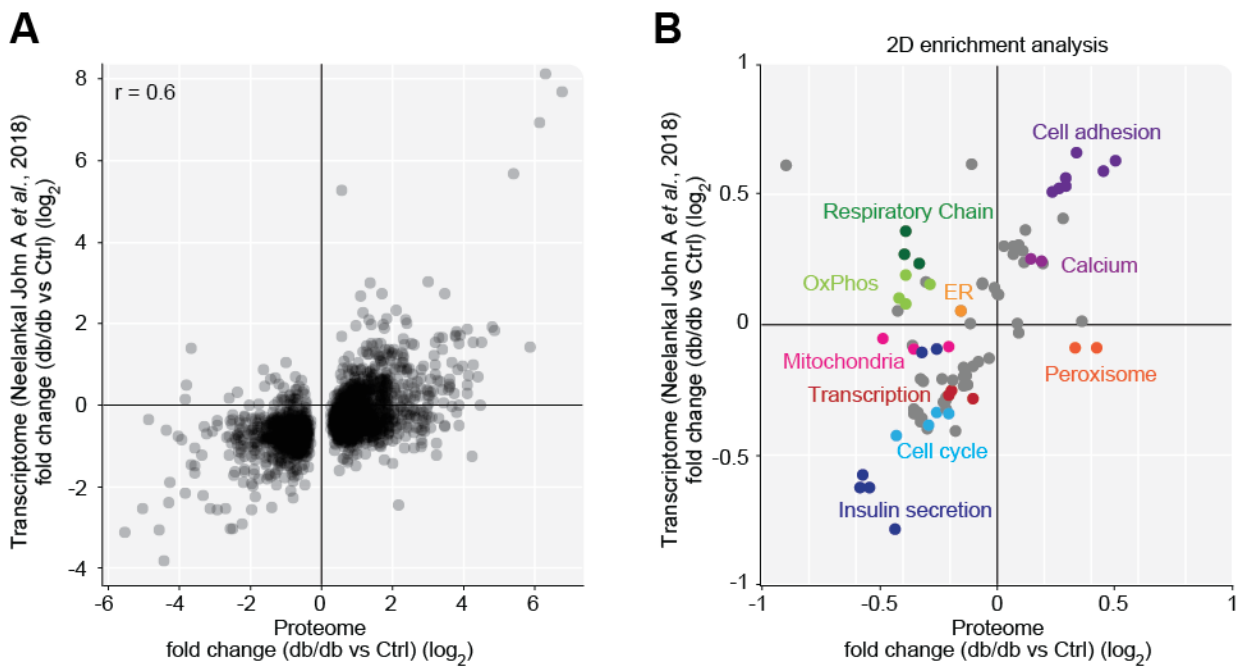


Figure S7, related to Figure 2

Identification of significantly modulated proteins and phosphosites. Statistically significantly up- and down-regulated proteins (A) and phosphosites (B) were identified by t-test (Benjamin Hochberg FDR < 0.07; S0=0.1) and represented as scatterplot. Each dot represents one protein (A) or one phosphosites (B). C) Enrichment and significance of GO-annotations, KEGG pathways and Keywords among the significantly modulated proteins.

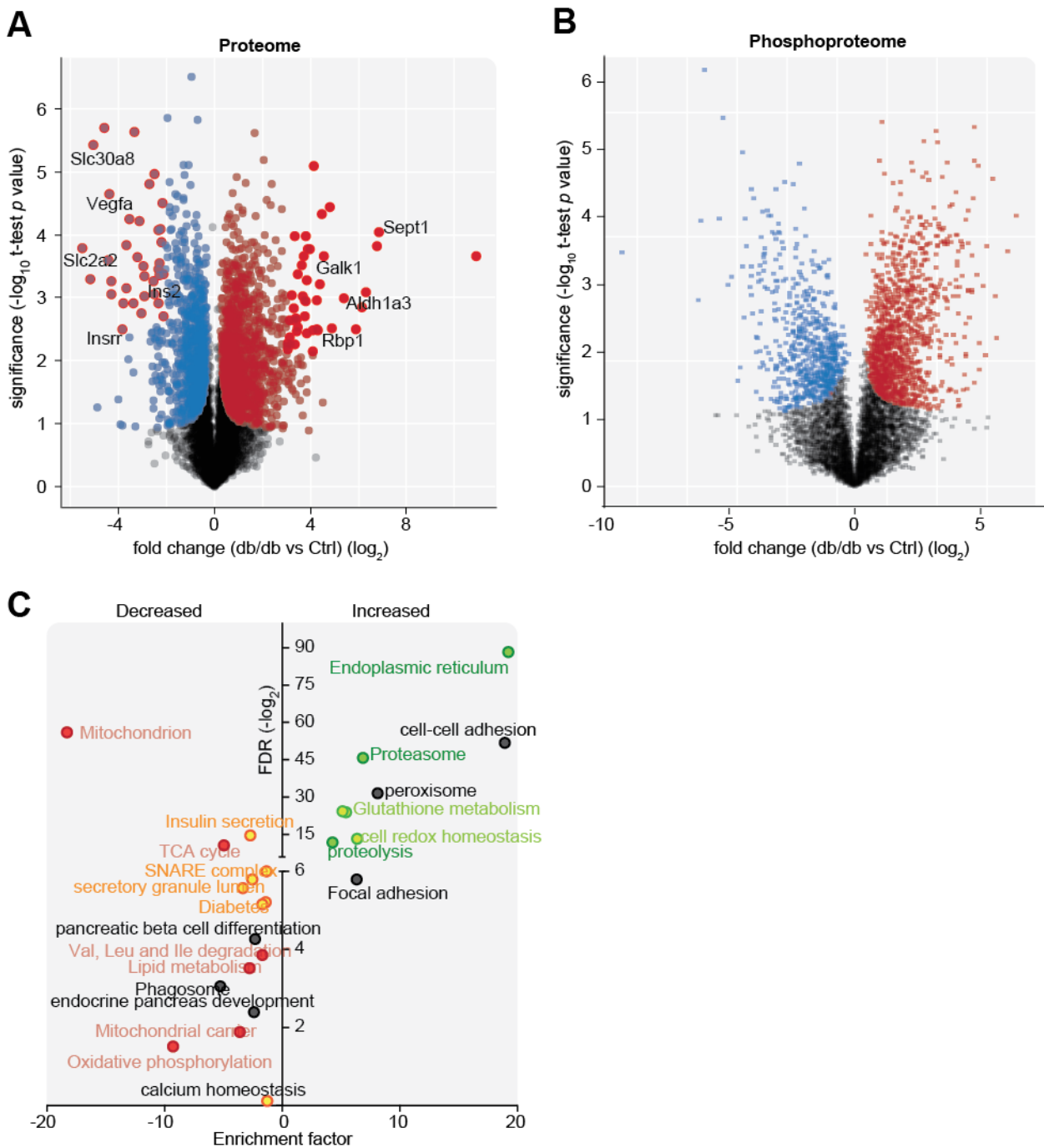


Figure S8, related to Figure 2

Key biological processes are regulated at the proteome and phosphoproteome levels. A) Pie chart indicating the percentage of positively and negatively modulated proteins (A), phosphosites (B) and phosphoproteins with at least one significantly modulated phosphopeptide (C). D) Percentage of phosphorylation sites with protein expression level quantified or not (left) and comparison between protein expression and phosphorylation levels for the 82% phosphorylation sites (right). Proteins and phosphorylation sites were considered regulated according to t-test analysis (FDR<0.07; S0=0.1). E) Plot showing the comparison of protein expression and phosphorylation level changes for the 39% phosphosites in (D, right). F) Clusters of GO term and Kegg pathways enriched in the subset of genes significantly up and down-regulated at the proteome and phosphoproteome level are represented as nodes of a co-citation network. Node size is correlated to the frequency of co-citation of each term with “islets” in literature abstract. Edge thickness is proportional to the “co-citation score”.

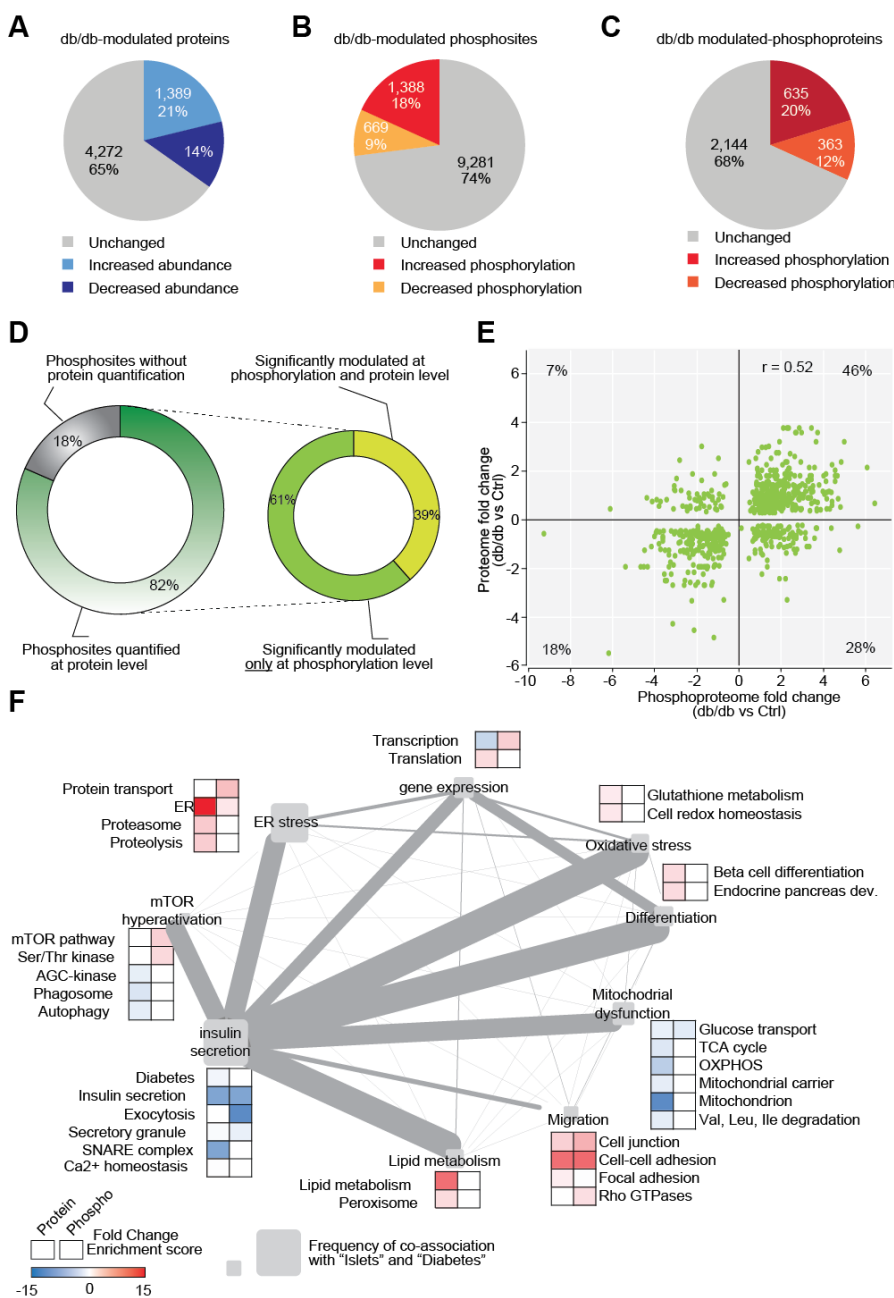


Figure S9, related to Figure 2

PDX1 phosphorylation in db/db islets. **A)** Intensity of the PDX1 phosphopeptide containing S269 (phosphoproteome dataset) normalized to the total protein intensity of the PDX1 protein (LFQ from proteome). **B)** mRNA level of PDX1 normalized on Tubulin and measured by qRT-PCR in db/db and Ctrl islets. **C)** LFQ intensity of PDX1 protein in db/db and Ctrl islets.

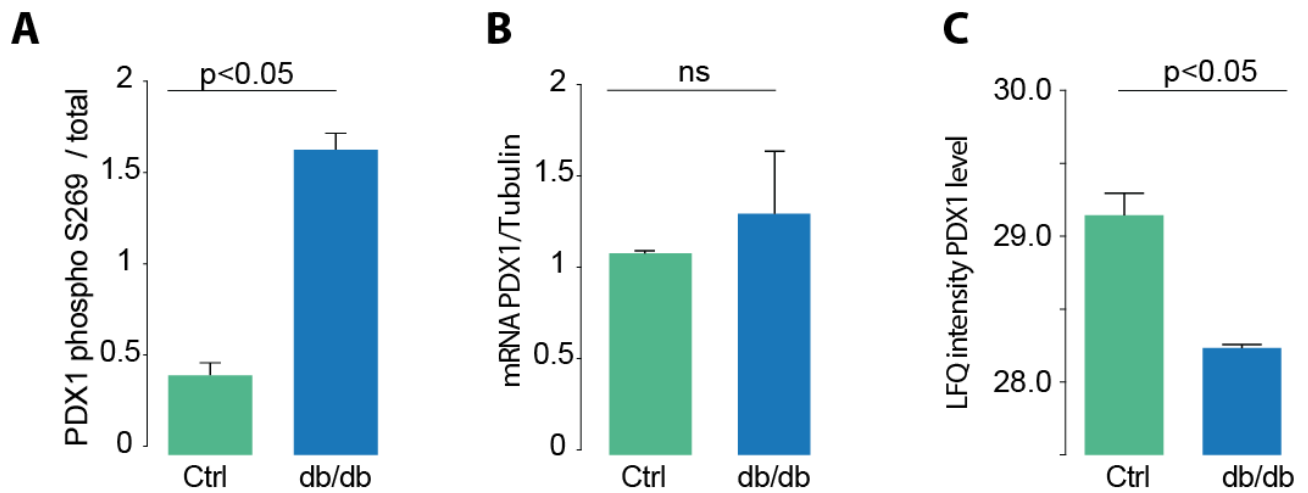


Figure S10, related to Figure 3

Islet cell type-specific markers are not affected in db/db islets. Expression change in db/db islets of 13 canonical literature-derived markers (A), of the most strongly differentially expressed markers identified by M.J. Muraro et al. (Cell Systems, 2016) (B) and of the most strongly differentially expressed markers identified by A. Segerstolpe et al. (Cell Metabolism, 2016) (D). C-E) Box plots of islets cell type specific literature-derived markers (M.J. Muraro et al, Cell Systems, 2016; A. Segerstolpe et al. Cell Metabolism, 2016) in diabetic islets compared to control islets.

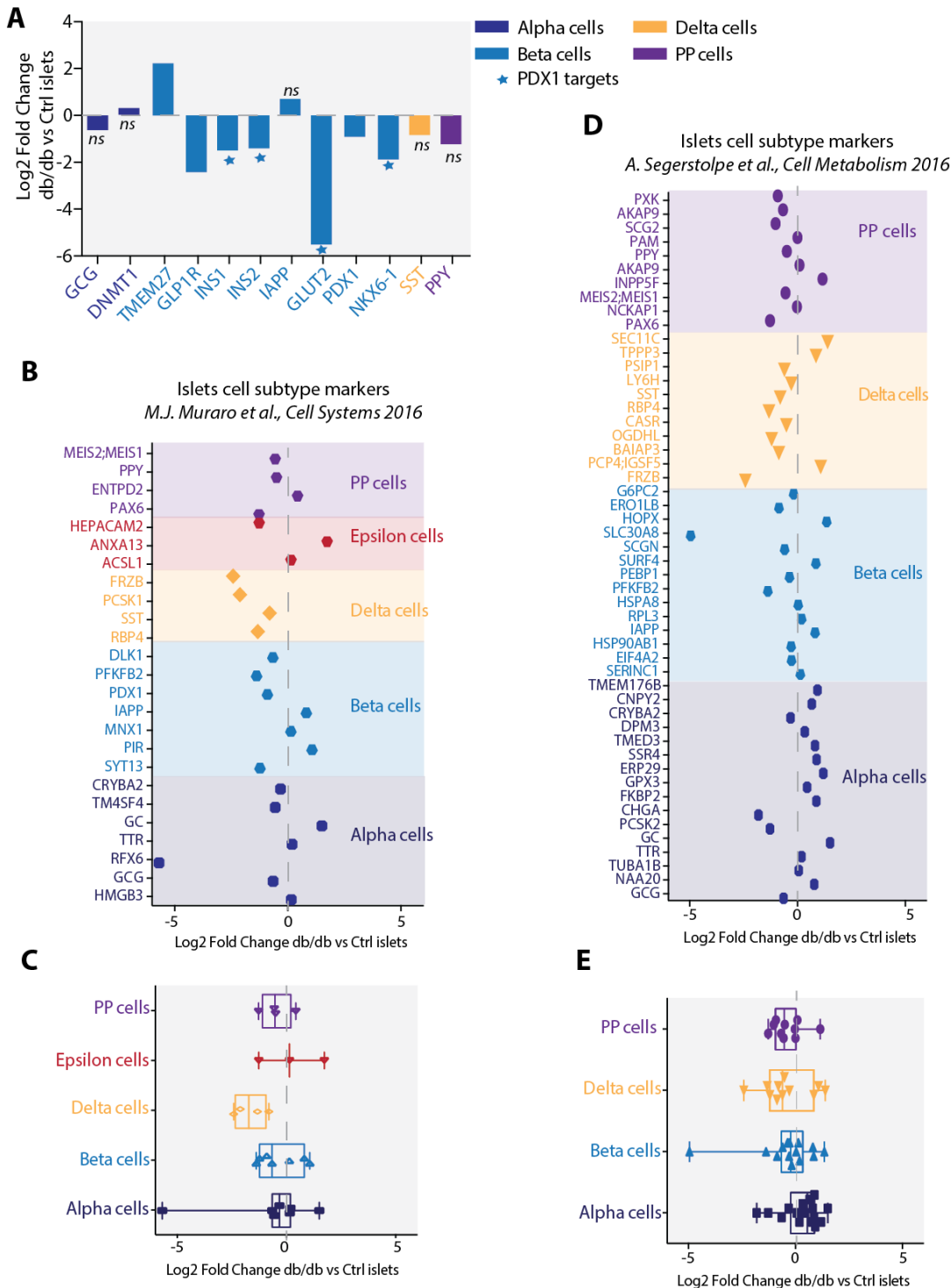


Figure S11, related to Figure 4

Reproducibility of biological replicates of proteome and phosphoproteome of glucose-treated INS1e cells. A) Schematic representation of the experimental workflow applied to analyze the proteome and phosphoproteome of INS1e cells after chronic high glucose stimulation. B) Proteome and phosphoproteome datasets were overlaid onto a literature-derived signaling network. C) Log₂ protein expression fold change of PDX1 and its transcriptional targets. D) Heatmap of the significantly modulated proteins in INS1e cells after chronic high glucose stimulation. Significantly enriched GO terms and pathways are indicated (FDR<0.07). Heat map showing the Pearson correlation coefficients between the different biological replicates in the proteome (E) and phosphoproteome (F) datasets.

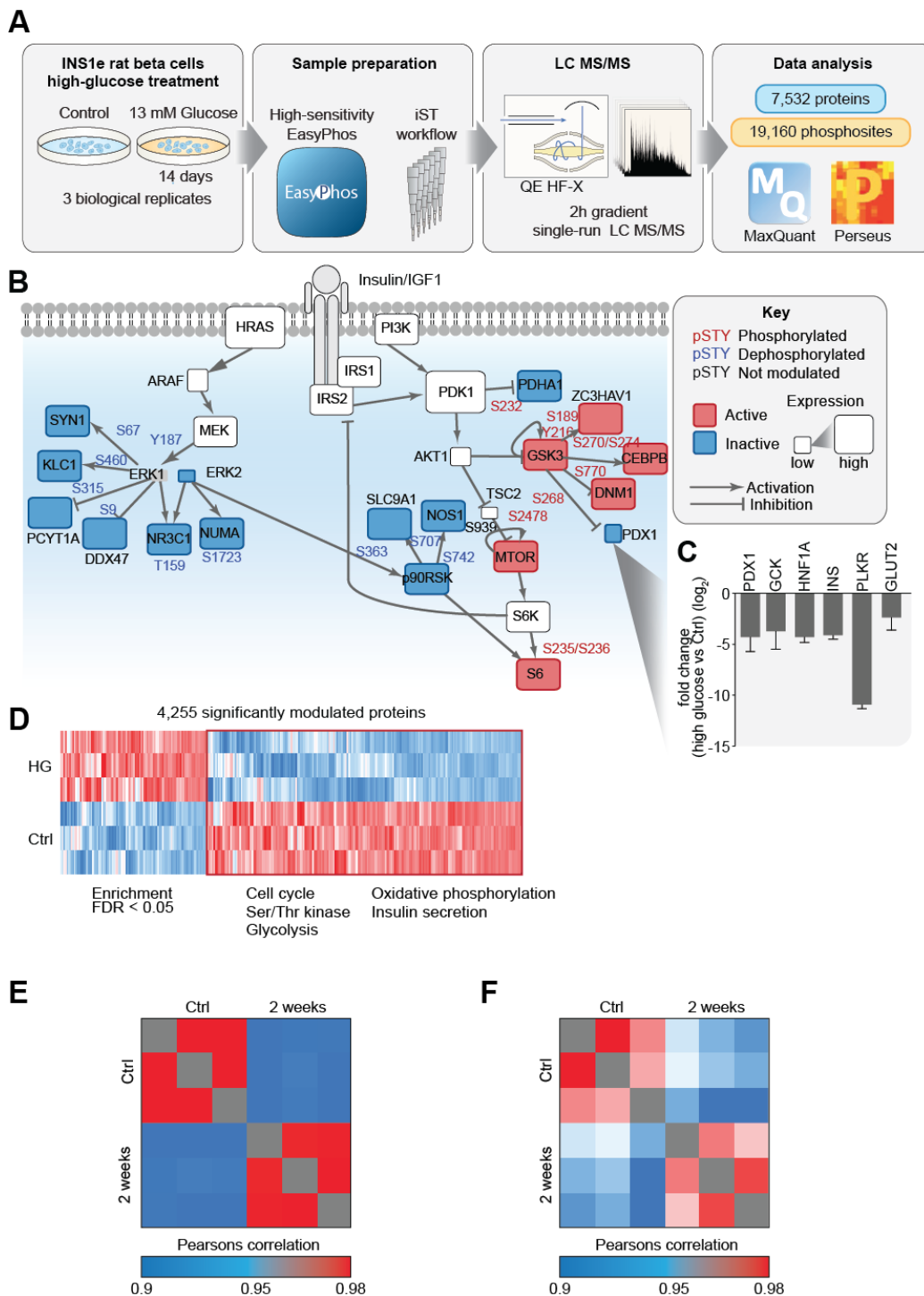


Figure S12, related to Figure 4

GSK3 activation impairs PDX1 and GLUT2 protein levels. Indirect immunofluorescent analysis of GLUT2 (A) GSK3 S9 (P) (B) PDX1 (C) with Phalloidin and DAPI in immortalized commercially available human islets treated with LY294002 (20 uM) in presence or in absence of MG132 (10 uM) or left untreated, as negative control.

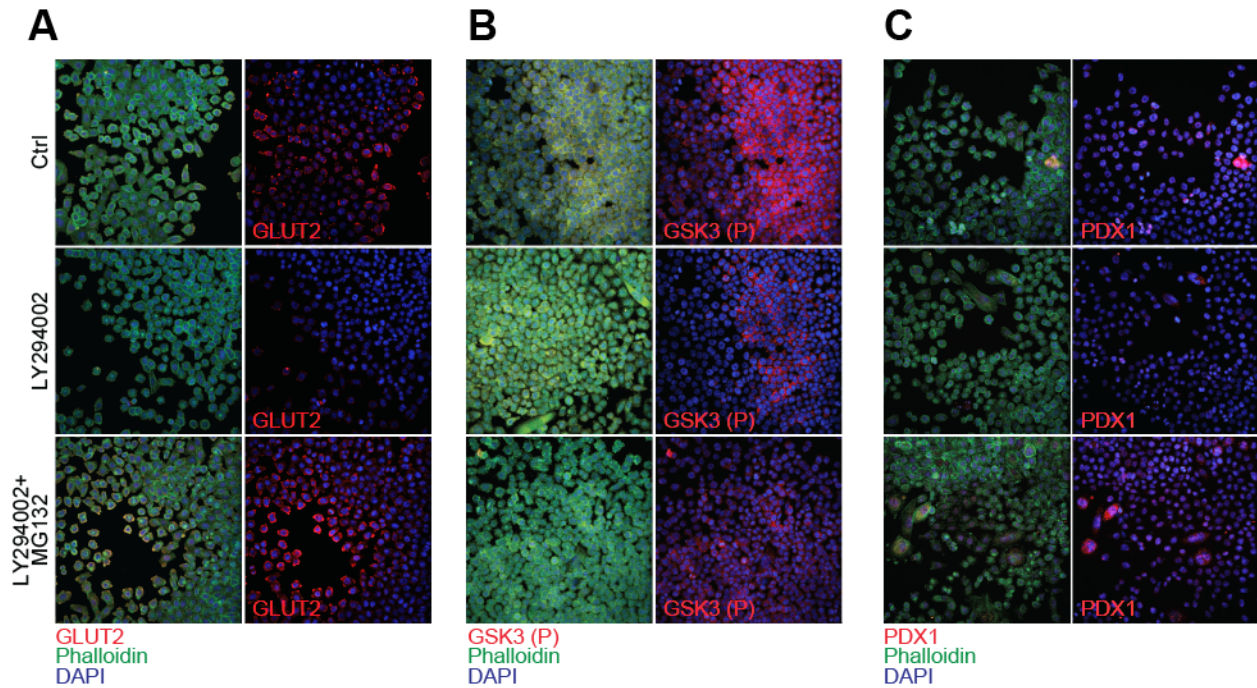
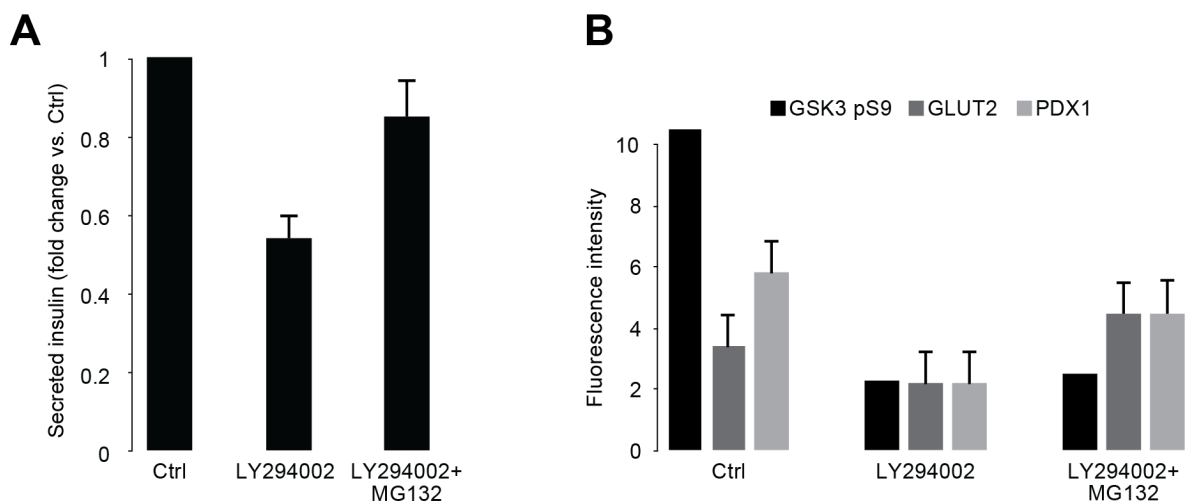


Figure S13, related to Figure 4

GSK3 activation impairs insulin secretion. A) Amount of secreted insulin after high glucose stimulation in commercially available human islets treated with LY294002 in presence or absence of MG132. B) Bar graph showing the immunofluorescent intensities of GSK3 S9 (P), GLUT2 and PDX1.



Secreted Insulin Raw Data (minus Blanck)												
	Ctrl				LY294002				LY294002 + MG132			
Low Glucose	2.68	2.59	5.36	10.33	0.49	6.23	1.31	4.73	7.14	2.04	5.88	2.05
High Glucose	6.26	8.56	9.82	15.34	0.49	7.30	1.47	5.53	13.93	3.60	9.06	3.44
Fold Change over Low Glucose stimulation												
	Ctrl				LY294002				LY294002 + MG132			
Low Glucose	1.00	1.00	1.00	1.00	1.00	1.00	1.00	1.00	1.00	1.00	1.00	1.00
High Glucose	2.33	3.31	1.83	1.48	1.00	1.17	1.12	1.17	1.95	1.76	1.54	1.68
Averaged data and statistical analysis												
	Ctrl	LY294002	LY294002 + MG132									
High/Low glucose	2.08	1.15	1.72	Median								
	0.79	0.08	0.17	St. Dev								
		0.02	0.03	pValues (vs Ctrl)								
				Student t Test								
Fold Change vs Ctrl	1.00	0.55	0.82									
		0.08	0.17	St. Dev								

Figure S14, related to Figure 4

GSK3 inhibition does not increase PDX1 mRNA level. Bar graph showing the mRNA level of PDX1 normalized on Tubulin and measured by qRT-PCR in biological triplicates (n=3) and technical duplicates.

